

Journal of
Mechanics of
Materials and Structures

**ELEMENT STACKING METHOD FOR TOPOLOGY OPTIMIZATION
WITH MATERIAL-DEPENDENT BOUNDARY AND LOADING
CONDITIONS**

Gil Ho Yoon, Yong Keun Park and Yoon Young Kim

Volume 2, N° 5

May 2007



mathematical sciences publishers

ELEMENT STACKING METHOD FOR TOPOLOGY OPTIMIZATION WITH MATERIAL-DEPENDENT BOUNDARY AND LOADING CONDITIONS

GIL HO YOON, YONG KEUN PARK AND YOON YOUNG KIM

A new topology optimization scheme, called the element stacking method, is developed to better handle design optimization involving material-dependent boundary conditions and selection of elements of different types. If these problems are solved by existing standard approaches, complicated finite element models or topology optimization reformulation may be necessary. The key idea of the proposed method is to stack multiple elements on the same discretization pixel and select a single or no element. In this method, stacked elements on the same pixel have the same coordinates but may have independent degrees of freedom. Some test problems are considered to check the effectiveness of the proposed stacking method

1. Introduction

This investigation is concerned with solving some class of topology optimization problems for which current formulations or modeling techniques are not easy to apply. When material-dependent boundary conditions need to be considered, current multimaterial approaches [Bendsøe and Kikuchi 1988; Stegmann and Lund 2005; Bendsøe and Sigmund 2003; Sigmund 2001; Yin and Ananthasuresh 2002; Mei and Wang 2004] may be difficult to apply directly. These problems may arise when only a particular material among a group of given materials is allowed along some specific boundaries because of assembly or mechanical/thermal impedance matching requirements.

Another difficult class of problems is to select not only material property but also element types governed by different field equations. For instance, one can consider design-dependent pressure load problems. These problems were solved by several approaches [Hammer and Olhoff 2000; Sigmund and Clausen 2007; Yoon et al. 2006], but a straightforward and easy-to-implement method may be useful.

In this investigation, we aim to develop an alternative method capable of dealing with the above-mentioned problems efficiently. The key idea in the proposed method is to stack multiple elements on the same discretization pixel. The number of the stacked elements at the same discretization pixel is the same as the number of candidate materials or material types. Though the nodes of stacked elements have exactly the same spatial coordinates, the nodal degrees of freedom need not to be the same. Consequently, elements of different types having different boundary or loading conditions can be stacked. When nonlinear elements are to be stacked, the element connectivity parameterization formulation [Yoon and Kim 2005a; 2005b] can be incorporated, but no nonlinear elements were considered in this work.

Keywords: element stacking, topology optimization, material-dependent boundary conditions.

For this research, the first author was supported by the Korea Research Foundation Grant funded by the Korean Government (MOEHRD, Basic Research Promotion Fund) (KRF-2004-214-M01-2004-000-20114-0).

After presenting the detailed modeling and implementation procedure of the proposed element stacking method, several verification problems are considered.

2. Element stacking method

2.1. Underlying concept and optimization formulation. Figure 1 compares multimaterial models by standard methods such as those of Stegmann and Lund 2005 and Yin and Ananthasuresh 2002, and by the proposed element stacking method. Unlike standard approaches using a single finite element, the element stacking method selects a finite element among elements satisfying different governing equations, or having different material properties subjected to different boundary conditions. Thus, more than one element is juxtaposed on the same pixel in the element stacking method. If only material selection is concerned, the element stacking method is basically the same as the standard multimaterial method.

To select only one finite element or a void from multiple elements, an element selection scheme should be used. Formulations for standard material selection can be used for element selection [Bendsøe and Sigmund 1999; Yin and Ananthasuresh 2002; Bendsøe and Sigmund 2003; Mei and Wang 2004; Stegmann and Lund 2005]. In this work, the following formulation by Stegmann and Lund 2005 will be modified for element selection needed in the stacking method:

$$C^e = \sum_{i=1}^{N_m} \left[(\gamma_i^e)^p \prod_{j=1}^{N_m} [1 - (\gamma_{j \neq i}^e)^q] \right] \bar{C}_i. \tag{1}$$

In Equation (1), the material property of the e th element is interpolated by those of available N_m materials. The design variable is γ_i^e ($0 < \gamma_i^e \leq 1$) to indicate the selection of the i th material at the e th element (if selected, $\gamma_i^e = 1$). The symbols (p, q) denote the penalty exponents. The actual material property of the i th material, such as Young’s modulus or thermal conductivity, is denoted by \bar{C}_i , and the corresponding material property for the e th element is denoted by C^e . The symbol Π in Equation (1) denotes a multiplication operator. For instance, if two materials, \bar{C}_1 and \bar{C}_2 , are considered, the following

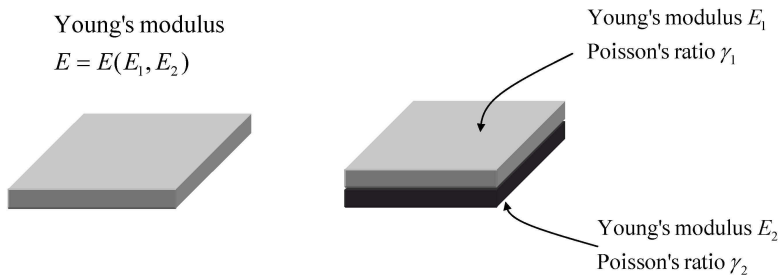


Figure 1. Left: multimaterial models by standard approaches using a single finite element. Right: the proposed element stacking method. Using the element stacking method, elements of different types and material-dependent boundary conditions can be handled. Without these conditions, the proposed method becomes identical to the standard multimaterial topology optimization.

interpolations are used:

$$C^e = \bar{C}_1(\gamma_1^e)^p(1 - (\gamma_2^e)^q) + \bar{C}_2(\gamma_2^e)^p(1 - (\gamma_1^e)^q) \quad (w_k = 1). \quad (2)$$

The interpolation formulation in Equation (1) is slightly modified so as to select the stiffness matrix \mathbf{k}^e of the e th pixel having N_m stacked finite elements, as

$$\mathbf{k}^e(\boldsymbol{\gamma}^e) = \mathbf{A}_{i=1}^{N_m} \mathbf{k}_i^e(\boldsymbol{\gamma}^e) = \mathbf{A}_{i=1}^{N_m} \phi_i^e(\boldsymbol{\gamma}^e) \bar{\mathbf{k}}_i^e = \mathbf{A}_{i=1}^{N_m} \underbrace{\left[(\gamma_i^e)^p \prod_{\substack{j=1 \\ j \neq i}}^{N_m} [1 - (\gamma_j^e)^q] \right]}_{\phi_i^e(\boldsymbol{\gamma}^e)} \bar{\mathbf{k}}_i^e, \quad (3)$$

where γ_i^e and ϕ_i^e denote the design variable and the participation factor of the i th element stiffness to the interpolated stiffness of the e th pixel, respectively. While the stiffness matrix $\mathbf{k}_i^e(\boldsymbol{\gamma}^e)$ depends on the set of design variables $\boldsymbol{\gamma}^e = \{\gamma_i^e, \gamma_i^e, \dots, \gamma_{N_m}^e\}^T$, the stiffness matrix $\bar{\mathbf{k}}_i^e(\gamma_i^e = 1, \text{ other } \gamma_{j, i \neq j}^e = 0)$ is a design variable-independent matrix. The pixel-level assembly operator of the element stiffness matrices \mathbf{k}_i^e is denoted by $\mathbf{A}_{i=1}^{N_m}$.

The main difference between formulas (1) and (3) is that the summation operator $\sum_{i=1}^{N_m}$ is replaced by the assembly operator $\mathbf{A}_{i=1}^{N_m}$. The stacked elements defined on the same pixel can have independent nodal degrees of freedom because a different boundary should be allowed to each of the stacked elements. Moreover, it is also possible to stack the differently formulated elements having same degrees of freedom. Therefore, the summation operator in (1) must be replaced by the element assembly operator in (3). In (3), two penalty parameters p and q are also used to improve solution convergence.

Notice that this element stacking method should have the identical effectiveness and numerical efficiency of the existing multimaterial design methods such as schemes presented in [Stegmann and Lund 2005] or [Yin and Ananthasuresh 2002] without the conditions presented in Figure 2. In other words, if only multiple-material problems are considered, there is no difference between the assembly operator $\mathbf{A}_{i=1}^{N_m}$ and the summation operator $\sum_{i=1}^{N_m}$. Thus, the same performance should be obtained between two methods which have the same interpolation functions.

For the case of compliance minimization, the following optimization setting is used while the interpolation formulation (3) is employed to implement the element stacking method:

$$\min_{\boldsymbol{\gamma}} F = \mathbf{u}^T \mathbf{f} \quad (4a)$$

$$\text{subject to } \mathbf{K}(\boldsymbol{\gamma})\mathbf{u} = \mathbf{f} \quad (4b)$$

$$m_i = \sum_{e=1}^{N_p} \gamma_i^e v^e \leq \bar{m}_i \quad \text{for } k = 1, \dots, N_m, \quad (4c)$$

where

$$\mathbf{K}(\boldsymbol{\gamma}) = \sum_{e=1}^{N_p} \mathbf{A} \mathbf{k}^e(\boldsymbol{\gamma}^e), \tag{4d}$$

$$\boldsymbol{\gamma} = \{\gamma^1, \gamma^2, \dots, \gamma^{N_p}\}, \quad \boldsymbol{\gamma}^e = \{\gamma_1^e, \gamma_2^e, \dots, \gamma_{N_m}^e\}, \tag{4e}$$

$$10^{-4} = \gamma_{\min} \leq \gamma_i^e \leq 1 \quad \text{for } i = 1, 2, \dots, N_m, \quad e = 1, 2, \dots, N_p. \tag{4f}$$

In Equation (4a), \mathbf{u} and \mathbf{f} are the nodal displacement vector and the nodal force vector, respectively. The global stiffness matrix is denoted by $\mathbf{K}(\boldsymbol{\gamma})$. The total number of discretizing pixels is N_p . The area or the volume of the e th pixel is denoted by v^e . Equation (4c) imposes the mass of the i th material to be bounded by \bar{m}_i . Thus, N_m mass constraints are used to constrain each of N_m materials.

To solve Equation (4) numerically, the method of moving asymptotes (MMA)¹ is employed [Svanberg 1987]. The sensitivity of the objective function $F(\boldsymbol{\gamma})$ with respect to the design variable γ_i^e can be written

$$\frac{\partial F}{\partial \gamma_k^e} = -(\mathbf{u}^e)^T \frac{\partial \mathbf{k}^e(\boldsymbol{\gamma}^e)}{\partial \gamma_k^e} \mathbf{u}^e, \tag{5}$$

where \mathbf{u}^e is the nodal displacement vector of the stacked finite elements defined on the e th pixel. The partial derivative $\partial \mathbf{k}^e(\boldsymbol{\gamma}^e)/\partial \gamma_k^e$ can be calculated explicitly from Equation (3) as

$$\begin{aligned} \frac{\partial \mathbf{k}^e(\boldsymbol{\gamma}^e)}{\partial \gamma_k^e} &= p(\gamma_k^e)^{p-1} \prod_{\substack{j=1 \\ j \neq k}}^{N_m} [1 - (\gamma_j^e)^q] \bar{\mathbf{k}}_k^e - q(\gamma_k^e)^{q-1} \sum_{\substack{i=1 \\ i \neq k}}^{N_m} \mathbf{A} \left[(\gamma_i^e)^p \prod_{\substack{j=1 \\ j \neq i, j \neq k}}^{N_m} [1 - (\gamma_j^e)^q] \right] \bar{\mathbf{k}}_i^e, \\ &= \frac{p}{\gamma_k^e} \phi_k^e(\boldsymbol{\gamma}^e) \bar{\mathbf{k}}_k^e - \frac{q(\gamma_k^e)^{q-1}}{1 - (\gamma_k^e)^q} \sum_{\substack{i=1 \\ i \neq k}}^{N_m} \phi_i^e(\boldsymbol{\gamma}^e) \bar{\mathbf{k}}_i^e. \end{aligned} \tag{6}$$

Substituting Equation (6) into (5) yields

$$\frac{\partial F}{\partial \gamma_k^e} = -\frac{p}{\gamma_k^e} (\mathbf{u}_k^e)^T \mathbf{k}_k^e(\boldsymbol{\gamma}^e) \mathbf{u}_k^e + \frac{q(\gamma_k^e)^{q-1}}{1 - (\gamma_k^e)^q} \sum_{\substack{i=1 \\ i \neq k}}^{N_m} (\mathbf{u}_i^e)^T \mathbf{k}_i^e(\boldsymbol{\gamma}^e) (\mathbf{u}_i^e), \tag{7}$$

where \mathbf{u}_k^e is the subset vector for \mathbf{k}_k^e from \mathbf{u}^e . The accuracy of the driven sensitivity is checked though the finite difference. Because the sensitivities of the constraint equations (4c) are trivial to derive, they will not be given here explicitly.

Because the problem under consideration is not a convex problem, the use of a gradient-based optimizer would yield local optima depending on different initial conditions and values of the penalty parameters. In numerical problems below, the best results are presented, not necessarily the global optima. Design variable filtering was also used. Specifically, the filtering radius is two times the element size.

2.2. Problems solved by element stacking method. Two classes of problems will be solved by the proposed element stacking method. When the element stacking method is applied to problems solved by existing methods, it can be used as an alternative and easy-to-implement method.

¹The authors thank Prof. Svanberg for providing his MMA code.

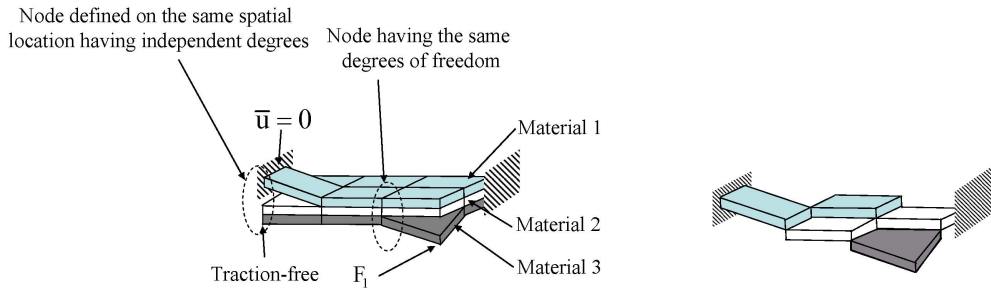


Figure 2. Element stacking modeling. Left: prescription of material-dependent boundary/loading conditions. Right: an optimized layout after topology optimization.

Class 1: Multiple materials and material-dependent boundary conditions. When material selection under material-independent boundary conditions is considered, the proposed element stacking formulation becomes virtually the same as the standard multimaterial selection formulation. Figure 2 (left) illustrates the case where material-dependent boundary conditions are prescribed, and Figure 2 (right) shows an optimal layout that may be obtained by the element stacking formulation. To deal with material-dependent conditions, the degrees of the nodes defined on the same spatial location are forced to be independent. Otherwise, they have the same degrees of freedom.

Class 2: Selection of elements of different types. An interesting application of the element stacking formulation is to select an element from a group of different elements, such as a solid elastic element and an incompressible fluid element. This may be solved as a material-selection problem, as demonstrated by Sigmund and Clausen 2007 and Yoon et al. 2006 for pressure-loaded structural design. Here, we will demonstrate that element stacking can be a simple and efficient alternative to solve the pressure-loaded structural design problem as well. For the element connectivity parameterization, the incompressible fluid is modeled by one element type (a mixed displacement-pressure element), and the solid by another (a nonconforming element). Example 4 presented in the next section deals with this problem.

3. Numerical results

In this section, four design examples are considered. Where applicable, results of the standard multimaterial approach are compared with those obtained with the stacking approach.

Example 1: Material-dependent boundary condition — compliance minimization case 1. To compare the element stacking method with the existing multimaterial design, the compliance minimization problem with simple material dependent boundary condition as shown in Figure 3 is considered. At the left-bottom and right-bottom sides, clamp boundary conditions are imposed only for the weak material and strong material, respectively. Though the problem involves material-dependent boundary conditions, one may consider using the existing multimaterial modeling technique depicted in Figure 4 (top).² Because

²The comparison of the existing multimaterial formulation with the element stacking method has been suggested by an anonymous reviewer.

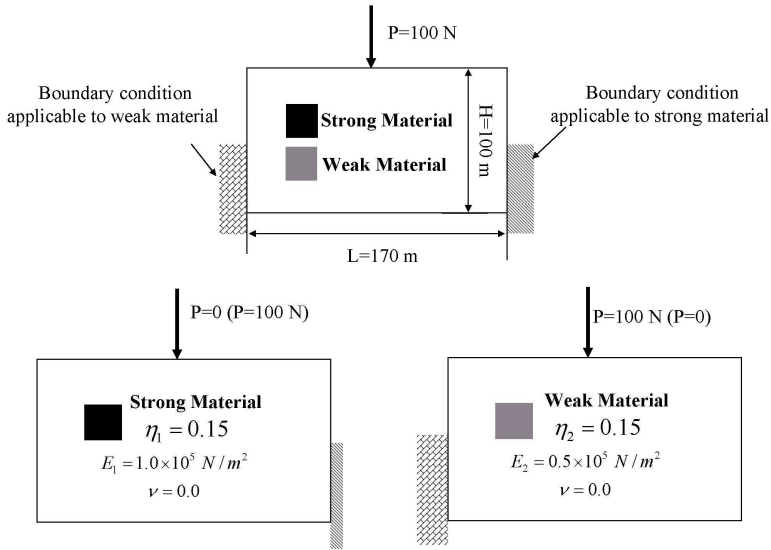


Figure 3. Compliance minimization problem involving material-dependent boundary conditions. Overall problem description (170 by 100 discretization) (top), conditions for Material 1 (strong material) (bottom left), and conditions for Material 2 (weak material) (bottom right). The permitted mass usage of Material i having Young’s modulus of E_i ($i = 1, 2$) is expressed by $\eta_i = \bar{m}_i/M$ where M is the mass of the material occupying the given design domain.

only Material 1 (strong material) is allowed to appear along the right lower side, $\gamma_2 = 0$ is used in the elements adjacent to the side. Similar modeling is used in the elements adjacent to the left lower side. When the element stacking method is used, two elements having materials 1 and 2 are juxtaposed on every pixel. Thus two layers of elements are placed on the design domain. In this modeling, only the nodes along the left and right lower sides with material-dependent boundary conditions have independent degrees of freedom. Thus, the system matrix size by the element stacking formulation is slightly larger than that of the standard multimaterial formulation. (Because the design domain is discretized by 171×101 elements, the size increases from $2 \times 171 \times 101$ to $2 \times 171 \times 101 + 2 \times 101$.)

The optimized layouts and the values of the objective function are shown in Figure 4.³ Because a gradient-based optimizer is used, optimal solutions tend to be affected by initial conditions. Therefore, presetting γ_i along the left and right lower sides in the existing multimaterial formulation tends to yield a local optimum having a poor objective function value. On the other hand, because the element stacking method does not preset γ_i along the sides, it appears easier for the local optimizer to find a better optimal solution. Although the result by the stacking method is also a local optimum (as evident from the presence of a small stiff material in the lower left part), Figure 4 indicates the advantage of using the element stacking formulation.

³To plot the results, we render the gray level of an optimized image proportional to $E_1 \times \gamma_1^e \times (1 - \gamma_2^e) + E_2 \times \gamma_2^e \times (1 - \gamma_1^e)$.

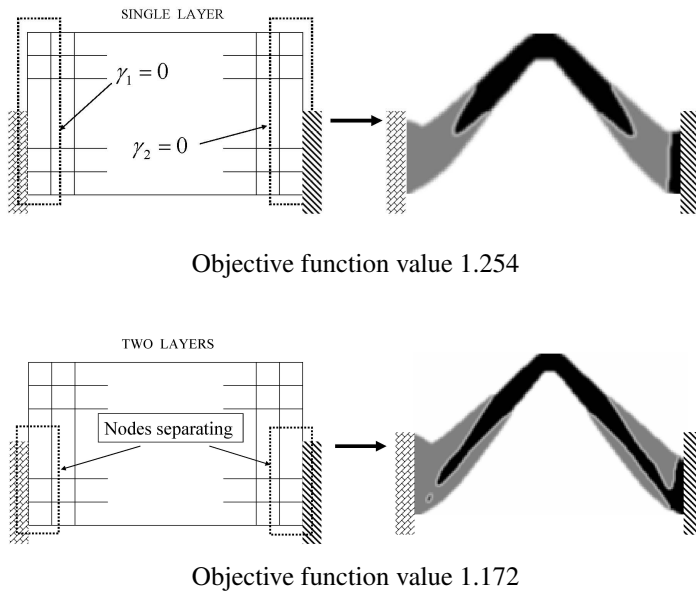


Figure 4. Top: optimization results for the problem design in Figure 3 by the standard mutlimaterial design method (where symbols γ_1 and γ_2 denote the design variables associated with strong and weak materials, respectively). Bottom: the element stacking method ($p = 5, q = 1$). A better result was obtained by the element stacking method.

Example 2: Material-dependent boundary condition — compliance minimization case 2. Figure 5 (top) shows another design problem involving complex material-dependent boundary conditions. The right lower boundary side constrains vertical displacement if strong material (Material 1) appears and horizontal displacement if weak material (Material 2) appears. This problem is made to demonstrate the potential use of the element stacking method because it is nearly impossible to solve by the existing multimaterial formulation. However, this problem is easy to handle with the proposed element stacking method. A similar problem having different boundary conditions is also considered in Figure 5 (bottom). Good convergence was observed in the optimal layout shown in Figure 5 (top).

Example 3: Two-material heat dissipating structure design. The topology optimization of an optimal two-material heat-dissipating structure, illustrated in Figure 6, is also considered. Though this problem has been solved by different approaches, it is interesting to demonstrate the effectiveness of the element stacking method in two-material heat dissipating structure design problems. For the optimization, both normal and side convection phenomena are taken into account.

To solve this problem, Equations (4a)–(4f) can be used as long as Equation (4b) is replaced by

$$[\mathbf{K}_T(\boldsymbol{\gamma}) + \mathbf{K}_h(\boldsymbol{\gamma})]\mathbf{u} = \mathbf{f} + \hat{\mathbf{f}}. \tag{8}$$

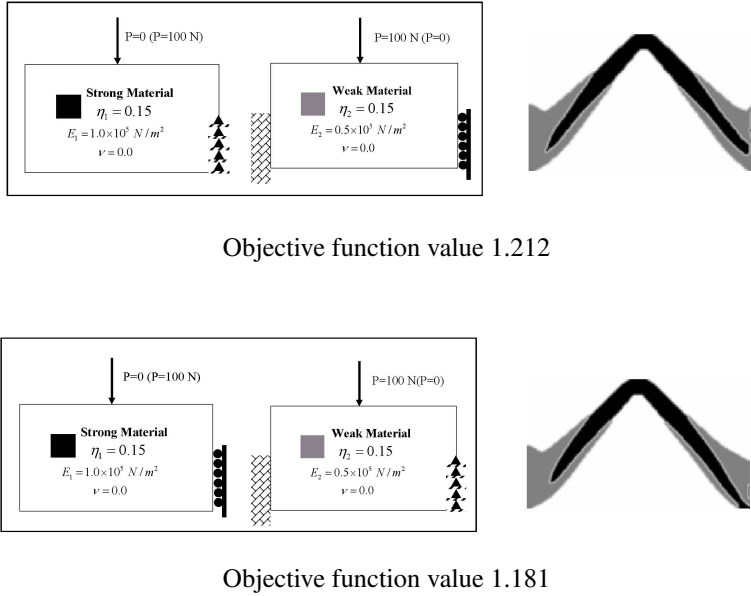


Figure 5. Compliance minimization problems involving material-dependent boundary conditions—Case 2. The boundary conditions for problems shown here in top and bottom are different. (The values of $p = 5$ and $q = 1$ were used.)

For the present problem, the symbols in Equation (4) and Equation (8) should be interpreted as

- $\mathbf{K}_T(\boldsymbol{\gamma})$: stiffness matrix of conductivity,
- $\mathbf{K}_h(\boldsymbol{\gamma}) = \mathbf{K}_{h_n}(\boldsymbol{\gamma}) + \mathbf{K}_{h_s}(\boldsymbol{\gamma})$: stiffness matrix of convection
= normal convection matrix + side convection matrix,
- $\hat{\mathbf{f}}$: nodal point heat flow input vector,
- \mathbf{f} : nodal vector due to the convection boundary condition,
- \mathbf{u} : nodal temperature vector.

Since the procedure to construct \mathbf{K}_T (all $\gamma_i = 1$), \mathbf{K}_h (all $\gamma_i = 1$), $\hat{\mathbf{f}}$ and \mathbf{f} is well known [Bathe 1996], it will not be given here. The formulation in Equation (3) is used to interpolate the element-level conductivity and convection matrices. Especially for the side convection interpolation, the amount of side convection occurring in the i th stacked element of the e th pixel is assumed to be proportional to its own participation factor $\phi_i^e(\boldsymbol{\gamma}^e)$, to facilitate sensitivity analysis; see Figure 7 (top). Figure 7 (bottom) shows a specific case. If the values of the variables are same for the stacked elements having the same material property, the net convection will vanish.

The optimized result for $k_1 = 10$, $k_2 = 1$, $h = 0.002$, $T_\infty = 0$ (room temperature), and $\hat{f} = 0.5$ is shown in Figure 8. The appearance of Material 1 near the heat input boundary physically makes sense because Material 1 has a higher conductivity.

Let us compare the optimized results for one-material optimization and the above two-material optimization. The results are compared in Figure 9. Note that the optimized result using Material 1 alone and the result using Material 2 alone are different because the ratio of the convection coefficient to the conductivity is different depending on the selected material. It is apparent that the performance of the optimized two-material structure behaves somewhere between that of Material 1 and that of Material 2.

Example 4: Design-dependent pressure-loaded problem. The design-dependent pressure-loaded problem is an interesting problem that has received some attention in the topology optimization community [Hammer and Olhoff 2000; Sigmund and Clausen 2007; Yoon et al. 2006]. Figure 10 (top) depicts the problem under consideration. The objective is to find an optimal structural layout in the design domain under pressure load. This can be solved as a material-selection problem [Sigmund and Clausen 2007; Yoon et al. 2006], but it is considered to demonstrate that the element stacking method is capable of handling different material element types. Thus, two different elements, one a mixed finite element capable of simulating incompressible fluid and the other a structural element, will be juxtaposed on the same pixel.

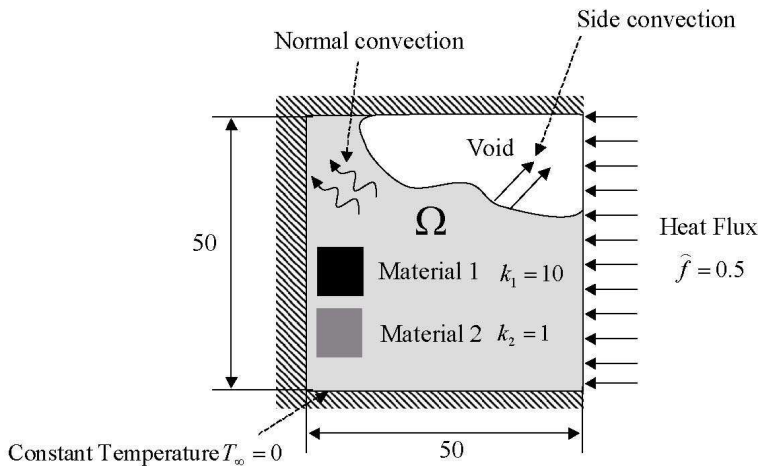


Figure 6. Problem definition for the two-material topology optimization of a heat dissipating structure. (Meshed by 50 by 50 finite elements. The materials are assumed to have different thermal conductivities k_i , but the same convection coefficient h . Heat flux input along the right side is $\hat{f} = 0.5$.)

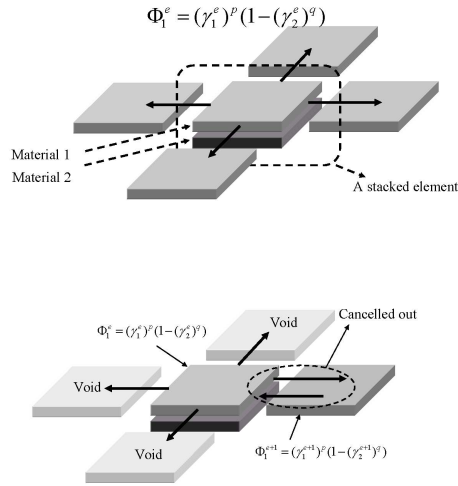


Figure 7. Side convection phenomenon modeled by the participation factor $\phi_i^e(\boldsymbol{\gamma}^e)$. Modeling concept (top), and a specific case where a stacked element in the center is interfaced with three void elements and one nonvoid element (bottom). In the bottom diagram, if γ_i^e are close to γ_i^{e+1} , the net side convection will virtually vanish.

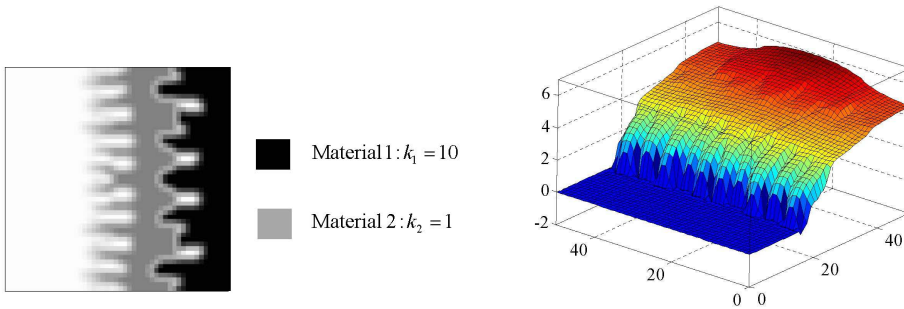


Figure 8. Optimized result for Problem 3 ($k_1 = 10$, $k_2 = 1$, $h = 0.002$, $T_\infty = 0$, $\hat{f} = 0.5$). Optimal distribution of two materials (top), and the temperature distribution of the optimized structure (bottom).

A mixed displacement-pressure element to simulate incompressible fluid ⁴ is the element used in Sigmund and Clausen 2007 and Yoon et al. 2006, which uses bilinear displacements field and constant pressure field. The shape functions in the natural coordinates are illustrated in Figure 11 (left). The structural element employed is a nonconforming element whose six shape functions are plotted in Figure 11 (right). Though other element types can be used, the stacking procedure may be best described with

⁴Any element expressing an incompressible fluid element can be used; we simply use the mixed element available from earlier works [Yoon et al. 2006].

these elements because they have different degrees of freedom. Equation (3) is also used to interpolate

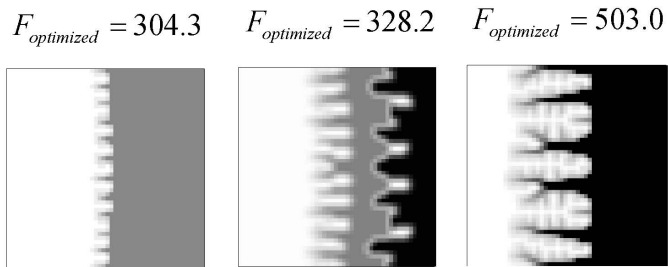


Figure 9. Comparison of the optimized results for Problem 3 using Left: only Material 1 ($k_1 = 1, \eta_1 = 50\%$); middle: both Material 1 ($k_1 = 10, \eta_1 = 25\%$) and Material 2 ($k_2 = 1, \eta_2 = 25\%$); and right: only Material 2 ($k_2 = 10, \eta_2 = 50\%$).

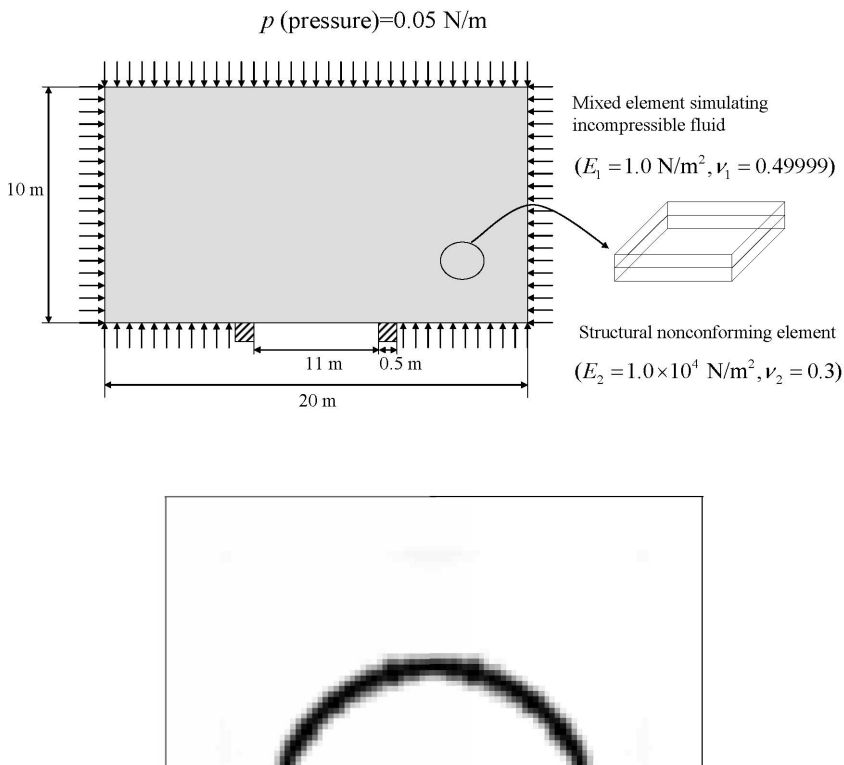


Figure 10. The pressure loaded structure design using the element stacking method. Top: problem description: discretization by 200×100 pixels, 5% structural mass constraint ratio; bottom: an optimization result.

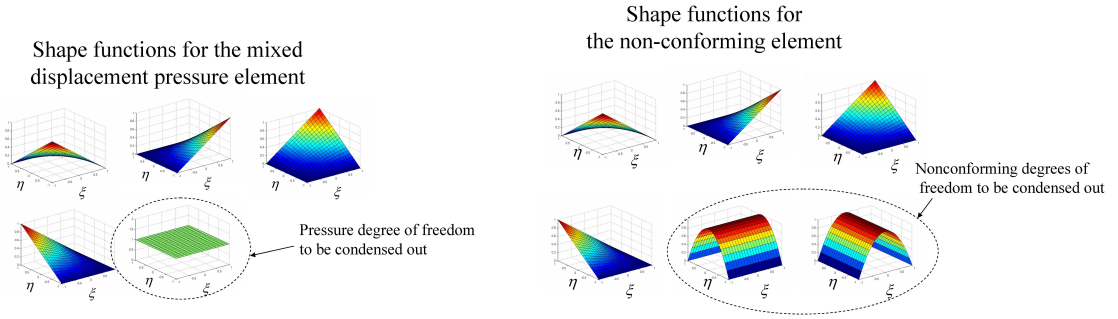


Figure 11. The employed shape functions in the local coordinators for the pressure loaded problem. Left: shape functions used for the mixed displacement-pressure element. Right: shape functions for the nonconforming element. (ξ, η : natural coordinates.)

the element stiffness matrices with the participation factor in Equation (10), as

$$k^e(\gamma^e) = \sum_{i=1}^2 \phi_i^e(\gamma^e) \bar{k}_i^e \tag{9}$$

- \bar{k}_1^e : stiffness matrix of the structural element,
- \bar{k}_2^e : stiffness matrix of the incompressible fluid element.

The participation factors $\phi_i^e(\gamma^e)$ in Equation (9) are given by

$$\phi_1^e(\gamma^e) = \frac{\gamma_1^e}{1 + (1 - \gamma_1^e)\alpha}, \quad \phi_2^e(\gamma^e) = 1 - \phi_1^e(\gamma^e), \tag{10}$$

where α is a penalization factor ($\alpha = 200$ was used in this work).

Because different degrees of freedom are used in the mixed element and the nonconforming element, the degrees of freedom not directly associated with nodes are condensed before the assembly procedure in Equation (9). Figure 10 (bottom) shows the optimized result by the element stacking method. Except for element stacking, no special numerical treatment was conducted to obtain the result. Though not explicitly shown, the result agrees well with results obtained earlier by other methods [Hammer and Olhoff 2000; Sigmund and Clausen 2007; Yoon et al. 2006].

4. Conclusions

A method to stack multiple elements on the same discretization pixel was developed to deal with topology optimization involving material-dependent boundary conditions. By making nodal degrees of freedom of the stacked elements on the same pixel independent, material-dependent boundary conditions were handled in the topology optimization setting. The usefulness of the stacking idea was demonstrated in a two-material heat dissipating structure design problem and also in a design-dependent pressure load problem. The latter problem was solved by simple stacking of an incompressible fluid element and an

elastic solid element with internal degree-of-freedom condensation. The stacking idea can be useful for topology optimization problems involving multiphase problems involving more than one physical principle.

References

- [Bathe 1996] K. J. Bathe, *Finite element procedures*, Prentice-Hall, New Jersey, 1996.
- [Bendsøe and Kikuchi 1988] M. P. Bendsøe and N. Kikuchi, “Generating optimal topologies in structural design using a homogenization method”, *Comput. Methods Appl. Mech. Eng.* **71**:2 (1988), 197–224.
- [Bendsøe and Sigmund 1999] M. P. Bendsøe and O. Sigmund, “Material interpolation schemes in topology optimization”, *Arch. Appl. Mech.* **69**:9-10 (1999), 635–654.
- [Bendsøe and Sigmund 2003] M. P. Bendsøe and O. Sigmund, *Topology optimization: theory, methods and applications*, Springer-Verlag, New York, 2003.
- [Hammer and Olhoff 2000] V. B. Hammer and N. Olhoff, “Topology optimization of continuum structures subjected to pressure loading”, *Struct. Multidiscip. O.* **19**:2 (2000), 85–92.
- [Mei and Wang 2004] Y. Mei and X. Wang, “A level set method for structural topology optimization and its applications”, *Adv. Eng. Softw.* **35**:7 (2004), 415–441.
- [Sigmund 2001] O. Sigmund, “Design of multiphysics actuators using topology optimization — part II: two-material structures”, *Comput. Methods Appl. Mech. Eng.* **190**:49-50 (2001), 6605–6627.
- [Sigmund and Clausen 2007] O. Sigmund and P. M. Clausen, “Topology optimization using a mixed formulation: an alternative way to solve pressure load problems”, *Comput. Methods Appl. Mech. Eng.* **196**:13–16 (2007), 1874–1889.
- [Stegmann and Lund 2005] J. Stegmann and E. Lund, “Discrete material optimization of general composite shell structures”, *Int. J. Numer. Methods Eng.* **62**:14 (2005), 2009–2027.
- [Svanberg 1987] K. Svanberg, “The method of moving asymptotes — a new method for structural optimization”, *Int. J. Numer. Methods Eng.* **24**:2 (1987), 359–373.
- [Yin and Ananthasuresh 2002] L. Yin and G. K. Ananthasuresh, “A novel topology design scheme for the multi-physics problems of electro-thermally actuated compliant micromechanisms”, *Sens. Actuators A Phys.* **97-98** (2002), 599–609.
- [Yoon and Kim 2005a] G. H. Yoon and Y. Y. Kim, “Element connectivity parameterization for topology optimization of geometrically nonlinear structures”, *Int. J. Solids Struct.* **42**:7 (2005), 1983–2009.
- [Yoon and Kim 2005b] G. H. Yoon and Y. Y. Kim, “The element connectivity parameterization formulation for the topology design optimization of multiphysics systems”, *Int. J. Numer. Methods Eng.* **64**:12 (2005), 1649–1677.
- [Yoon et al. 2006] G. H. Yoon, J. S. Jensen, and O. Sigmund, “Topology optimization of acoustic-structure interaction problems using a mixed finite element formulation”, *Int. J. Numer. Methods Eng.* (2006).

Received 19 May 2006. Accepted 27 Jan 2007.

GIL HO YOON: ghy@mek.dtu.dk

Department of Mechanical Engineering, Solid Mechanics, Nils Koppels Allé, Building 403, DK-2800 Kgs. Lyngby, Technical University of Denmark, Denmark

YONG KEUN PARK: ykpark@mit.edu

Department of Mechanical Engineering, Massachusetts Institute of Technology, 77 Massachusetts Avenue, Cambridge, MA 02139-4307, United States

YOON YOUNG KIM: yykim@snu.ac.kr

Multiscale Design Center and Integrated Design & Analysis of Structures Laboratory, School of Mechanical and Aerospace Engineering, Seoul National University, Kwanak-Gu San 56-1, Seoul 151-742, Korea